# Comparison between $Nb_3Al$ and $Nb_3Sn$ Strands and Cables for High Field Accelerator Magnets

Ryuji Yamada, Akihiro Kikuchi, Emanuela Barzi, Guram Chlachidze, Allen Rusy, Takao Takeuchi, Michael Tartaglia, Daniel Turrioni, Vesselin Velev, Masayoshi Wake, and Alexander V. Zlobin

***Abstract*—The $Nb_3Al$ small racetrack magnet, SR07, has been successfully built and tested to its short sample limit beyond 10 Tesla without any training. Thus the practical application of $Nb_3Al$ strands for high field accelerator magnets is established. The characteristics of the representative F4 strand and cable, are compared with the typical $Nb_3Sn$ strand and cable. It is represented by the OST high current RRP $Nb_3Sn$ strand with 108/127 configuration. The effects of Rutherford cabling to both type strands are explained and the inherent problem of the $Nb_3Sn$ strand is discussed. Also the test results of two representative small racetrack magnets are compared from the stand point of Ic values, and training. The maximum current density of the $Nb_3Al$ strands is still smaller than that of the $Nb_3Sn$ strands, but if we take into account of the stress-strain characteristics, $Nb_3Al$ strands become somewhat favorable in some applications.**

***Index Terms*—$Nb_3Al$ Strand, $Nb_3Sn$ Strand, Rutherford Cable, Superconducting Magnet.**

## I. INTRODUCTION

THE copper stabilized $Nb_3Al$ strand with high current density was recently developed using the Rapid Heating/Quenching and Transformation method (RHQT) at NIMS [1]. With the successful production of Rutherford cables and successful tests of small magnets at Fermilab, the application of the $Nb_3Al$ strands for high field accelerator magnets became feasible [2]. Several different types of $Nb_3Al$ strands with different matrix material, such as Nb, Ta or Cu, have been developed and their characteristics were studied with regard to magnetization, instability and quench [2]-[4]. The most suitable strands, F3 and F4, for high field accelerator magnets were selected. The $Nb_3Al$ strand and its Rutherford cable has better strain tolerance than the counterparts made of $Nb_3Sn$ strand. The maximum current density of $Nb_3Al$ strand is still smaller than that of $Nb_3Sn$ strand, but if we take into account of stress-strain characteristics, $Nb_3Al$ strands become favorable in some applications.

Manuscript received 20 October 2009. This work was supported by the U.S. Department of Energy.

R. Yamada, E. Barzi, G. Chlachidze, A. Rusy, M. Tartaglia, D. Turrioni, V. Velev and A.V. Zlobin are with Fermi National Accelerator Laboratory, Batavia Illinois, 60510 USA (phone: 630-840-3660; fax: 630-840-3369; e-mail: yamada@fnal.gov).

A. Kikuchi and T. Takeuchi are with National Institute for Material Science (NIMS), 1-2-1 Sengen, Tsukuba, Ibaraki 305-0047, Japan.

M. Wake is with High Energy Accelerator Research Organization (KEK), 1-1 Oho, Tsukuba, Ibaraki 305-0801, Japan.

For the last decade, several different types of $Nb_3Sn$ strands were manufactured for, and have been successfully used for, high field accelerator magnets [5]. But it seems the $Nb_3Sn$ Rutherford cables are still in an R&D stage for the application to high field accelerator magnets, and not all magnets made with $Nb_3Sn$ are completely trouble free [6].

We compare the characteristics of these two A15 type materials, illustrate their strong and weak points, and consider some improvements when they are made into Rutherford cables. The major technically difficult points of the $Nb_3Sn$ strands are due to excessive deformation of the subelements during the fabrication of Rutherford cables, resulting in tin leakage, and/or joining together of subelements. In order to reduce $d_{eff}$, (the effective filament size), we make the filament size smaller, but it is not clear how far can we go without causing problems. We will discuss these problems in comparison with $Nb_3Al$ strands.

## II. $NB_3AL$ STRANDS AND RUTHERFORD CABLES

In the last several years, we have developed and tested four series F1, F2, F3 and F4 $Nb_3Al$ strands [1]. They are all copper stabilized 1 mm diameter $Nb_3Al$ strands. The differences are in the material of their central cores and the matrix between the subelements. F1 strand was made with Nb for both elements, and F1 was shown to be unstable at low field due to its huge magnetization caused by Nb components [3].

The best $Nb_3Al$ strands are presently the F3 and F4 series. Their metallurgical compositions are the same and Tantalum is used for both core and matrix. This composition was found the best for our application from the stability stand point. The cross sections of these strands are shown in Fig. 1 and 2. Their major characteristic parameters are shown in Table I together with those of a typical RRP $Nb_3Sn$ strand. The copper to non-copper ratio of F3 is 1.0, but that of F4 was reduced to 0.61 to increase its critical current Ic value.

In the following we will use the F3 strand as a typical $Nb_3Al$ strand to compare with a typical $Nb_3Sn$ strand.

### A. *Typical $Nb_3Al$ Strand F3*

The precursor of F3 strand is fabricated by the RHQT method, and electroplated at the speed of 5 m/hour. Its non-copper Jc is about 1500 A/mm$^2$ at 4.2 K at 12 Tesla. It has 222 subelements, and the $d_{eff}$ is 38 μm. Its cross section is shown in Fig. 1 and its characteristic parameters are shown in Table I.

The F3 magnetization curve is shown In Fig.3, which was measured with the integration method using a long sample. The relatively large downward loop at 1.9 K is caused by the outermost Nb layer, which is used to make a solid bonding to the electroplated copper stabilizer. This does not cause any instability with the magnet operation at 2.2 K, as explained later [2].

### *B. F3 and F4 Rutherford Cables*

The cross sections of the 27-strand Rutherford cables made of 1 mm diameter F3 and F4 strands, are shown in Fig. 4 and Fig. 5 respectively.

A close-up view of the strands at the narrow edge of the key stoned F3 Rutherford cable is shown in Fig. 6. As the precursor of $Nb_3Al$ is very hard, we observe hardly any deformation in it, while quite extensive deformation is observed in the copper stabilizer part. As bonding of the copper to the Nb surface is strong, there are no debonded regions nor any observable voids.

These pictures show that Rutherford cabling causes no significant distortion. This is related to the fact that the $Nb_3Al$ strands are quite strain-stress resistant as shown later.

TABLE I
$NB_3AL$ AND $NB_3SN$ ROUND STRAND SPECIFICATIONS

| Strand ID | F3 | F4 | RRP 108/127 |
|---|---|---|---|
| Magnet made and tested | SR05 (not tested) | SR07 | SR03 |
| Strand Dia. (with Cu) | 1.00 mm | 0.99 mm | 1.00 mm |
| Strand Dia. (w/o Cu) | 0.70 mm | 0.78 mm | 0.7 mm |
| No. of Subelements | 222 | 276 | 108 |
| No. of Total Subelements | 222 + 19 | 276 + 37 | 127 |
| Physical Filament Dia. | 38 μm | 35.8 μm | 67 μm |
| Cu/Non-Cu ratio | 1.0 | 0.61 | 1.17 |
| Inter-filament Matrix | Tantalum | Tantalum | Copper |
| Central Core of Strand | Tantalum | Tantalum | Copper |
| Central Core of Filament | Tantalum | Tantalum | Tin |
| Most-Outsider Matrix | Niobium | Niobium | ----- |
| Area Reduction (AR) | 71.6 % | 65.3 % | ----- |
| Cu Ion Plating Speed | 120 m/h | 120 m/h | ----- |
| Cu Electroplating Spd | 5 m/h | 7 m/h | ----- |
| $I_c$ (4.2 K, 12 T) | 581.3 A | 645.9 A | 925 A |
| $I_c$ (4.2 K, 15 T) | 343.0 A | 376.5 A | 474 A |
| non-Cu $J_c$(4.2 K,12 T) | 1,481 A/mm$^2$ | 1,352 A/mm$^2$ | 2,312 A/mm$^2$ |
| non-Cu $J_c$(4.2 K,15 T) | 874 A/mm$^2$ | 788 A/mm$^2$ | 1185 A/mm$^2$ |
| Ic Degradation due to Compression at 100/150 MPa (%) | ~ 0.0 /~0.0 | ~0.0 /~0.0 | ~15 / ~50 |
| n value (4.2 K,12 /15 T) | 49.9 / 40.3 | 40.0 / 34.3 | 33 / 27 |
| *RRR* (20K/300K) | 80-170 | 150-250 | 173 |
| Twist Pitch (mm) | 11-362, ∞ | 45 | 14 |

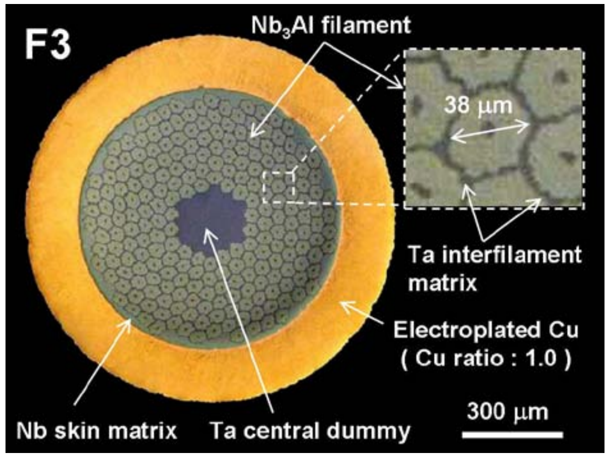

Fig. 1. Cross section of F3 $Nb_3Al$ strand. It has a Ta center core and Ta inter-filament matrix.

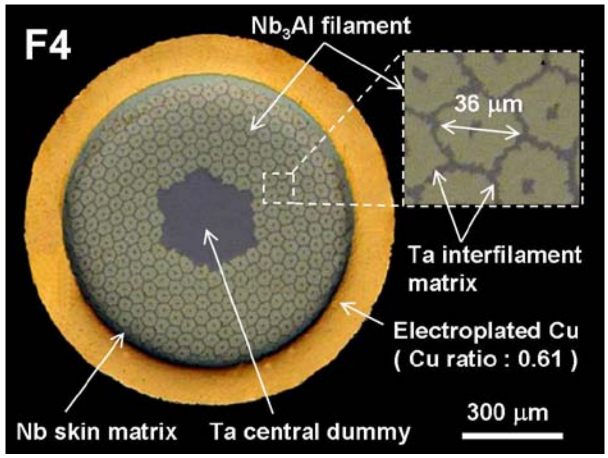

Fig. 2. Cross section of F4 $Nb_3Al$ strand. It has a Ta center core and Ta inter-filament matrix.

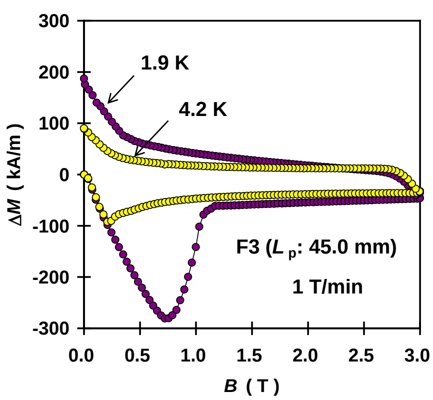

Fig. 3. Magnetization curves of F3 Ta matrix strand at 4.2 and 1.9 K.


Fig. 4. The cross section of a keystoned Rutherford cable made with 27 F3 $Nb_3Al$ strands, with a high compaction factor of 87.0 %.


Fig. 5. The Cross-section of a rectangular Rutherford cable made with 27 F4 $Nb_3Al$ strands, with a high compaction factor of 86.5 %. 13.95 x 1.85 mm$^2$.

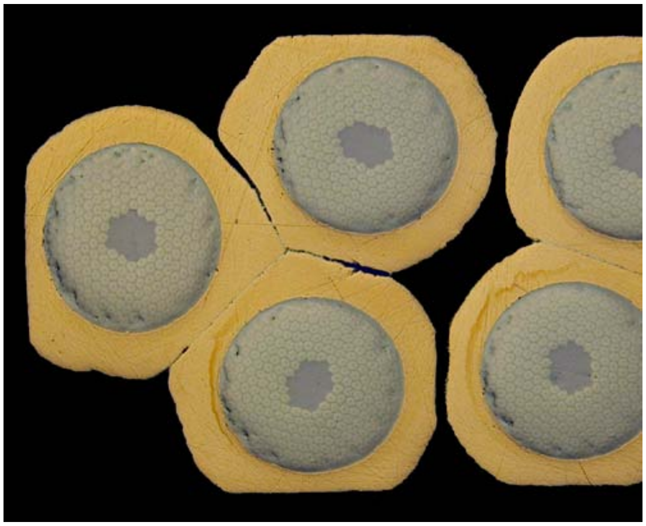

Fig. 6. Expanded cross section of F3 $Nb_3Al$ strands at the narrow edge of the keystoned Rutherford cable, which were used for the SR05 magnet. Copper stabilizer is plastically deformed, but the RHQT precursor is deformed only slightly. No debonding between the outermost Nb layer and the electroplated copper stabilizer is observed.

## III. $NB_3SN$ STRANDS AND RUTHERFORD CABLES

In the last decade, extensive studies on high current density $Nb_3Sn$ superconductors have been done in US and in Europe, both in laboratories and in industries [7]. The application for high field accelerator magnets, mostly using Rutherford cables made with internal tin $Nb_3Sn$ conductors, motivated these studies.

### *A. Typical $Nb_3Sn$ Strand RRP108/127*

Since Oxford Instruments Superconducting Technology developed the Restacked Rod Process (RRP), which achieved a non-copper Jc of 3000A/mm$^2$, their product with 54 subelements in the 61 stack prevailed in US laboratories [8]. There were several modifications to RRP: the RRP strand with 108 subelements in the 127 stack, with increased copper spacing is now in use in US laboratories [9]. The 108/127 strand cross section is shown in Fig. 7 and its characteristic parameters are listed in Table I.

### *B. Typical $Nb_3Sn$ Rutherford Cable*

The Rutherford cable made with OST RRP $Nb_3Sn$ strands with 108/127 configuration is shown in Fig. 8. This is a keystoned cable, and the expanded view of its strand at the right edge of the top layer is also shown. The original circular shapes of the subelements are now deformed into elongated shapes and some of the Nb layer components are merged with the neighboring subelements and/or broken open. This leads to the tin leak and effectively bigger magnetization, and instability of the magnets. With the old RRP 54/61 strands this deformation and damage was much worse. The effects of tin leakage on RRR and thermal conductivity and possible instability have been previously discussed [10]. Recently its experimental data was presented in [11].

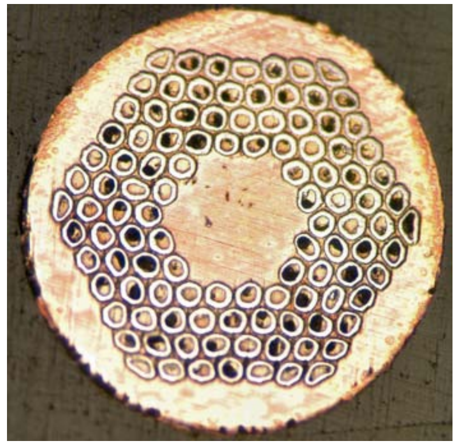

Fig. 7. Cross section of a typical heat-treated 1 mm dia. $Nb_3Sn$ strand, OST RRP 108/127 configuration with thick copper subelement ratio of 0.13. The black spots inside the subelements are voids.

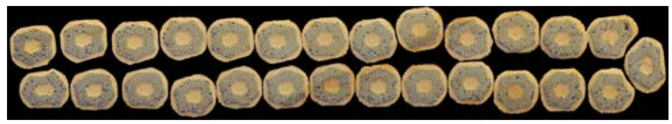

Fig. 8. Cross section of heat-treated keystoned Rutherford cable made with the RRP 108/127 $Nb_3Sn$ strands.

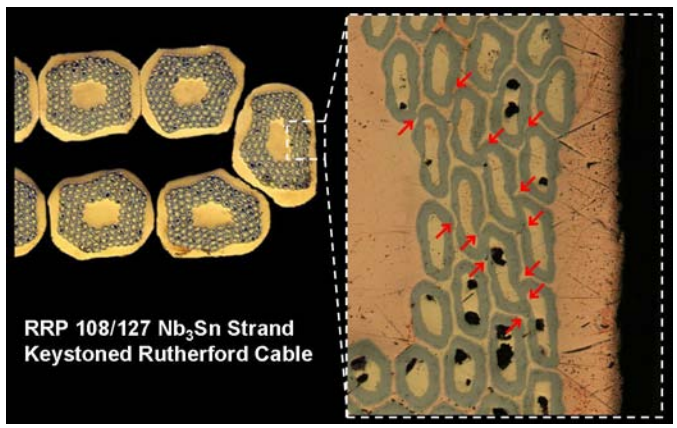


Fig. 9. Several strands at the edge of the Rutherford cable are shown at left. The inside of the edge strand is further expanded and shown at right. It is shown that some subelements are damaged and merged with their neighboring subelements. Voids are evident as black spots.

## IV. SENSITIVITY TO COMPRESSIVE FORCE ON STRANDS.

The test results for the compressive force are shown in Fig. 10 for F1 $Nb_3Al$ strand and the RRP $Nb_3Sn$ strand [1], [7]. The F1 $Nb_3Al$ strand was also made by the RHQT method and is expected to have similar hardness; we expect F3 and F4 $Nb_3Al$ to be harder than F1, because they have a Ta matrix instead of a Nb matrix. According to this data, $Nb_3Al$ strands can easily withstand 210 MP, while RRP $Nb_3Sn$ strands show 10 to 15 % degradation at 100 MPa in the short sample tests.

## V. SMALL RACETACK MAGNETS

Small racetrack magnets (SR) are used for quick testing of high current Rutherford cables made from newly developed superconducting strands [12]. In our standard design, a two–layer coil was wound from one piece of cable in the common coil configuration. It has a gap of 2 mm to achieve the highest field between two layers.

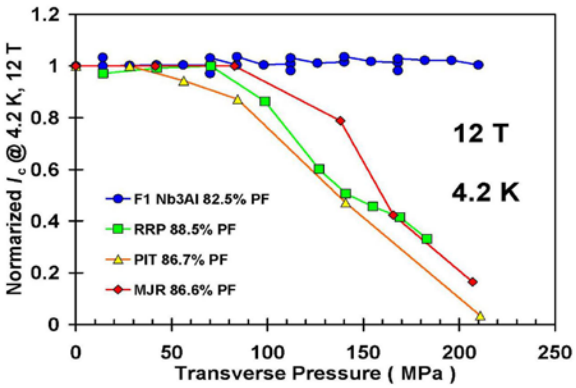


Fig. 10. Normalized critical current versus transverse pressure for F1 $Nb_3Al$ strand. The strand data from major $Nb_3Sn$ strands are also plotted from the reference [1] and [7].

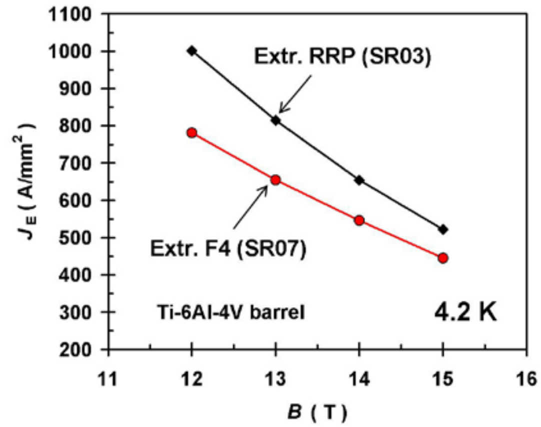


Fig. 11 Overall Jc for the extracted strands taken from F4-$Nb_3Al$, and RRP-$Nb_3Sn$ cables [11]. Those cables were used for small racetrack magnets of SR07 and SR03, respectively.

## A. *Maximum Fields of SR Magnets and $J_c$ and $I_c$ of Strands*

Test results of the $Nb_3Al$ small racetrack magnet SR07 [2], and two $Nb_3Sn$ RRP SR magnets are shown in Table II. The SR03 magnet was made from RRP strands with 108/127 configuration [13] and the SR06 with 114/127 configuration [14]. The maximum quench current values of SR03 and SR07 magnets are extrapolated data, because the power leads were quenching. All SR magnets are made of 13 turn/coil, except SR06, which is made of 12 turn/coil.

The test results of the SR07 $Nb_3Al$ magnet are reasonable compared to the SR03 $Nb_3Sn$ magnet data even though the Ic of $Nb_3Al$ strand is still low. There is 10 % difference between their maximum current values. The copper ratio of F4 $Nb_3Al$ strand was intentionally reduced to make its Ic value bigger.

The $Nb_3Sn$ RRP magnets, SR03 and SR06 achieved higher magnetic field than the $Nb_3Al$ magnet SR07 both at 4.5 K and 2.2 K operation. This fact is clearly explained by the higher Jc and Ic of RRP strands as shown in the Table I and Fig. 11.

The SR06 achieved a higher field than the SR03 at 4.5 K operation, but not at 2.2 K operation. This is due to the slight damages in the strands of the SR06 during its cabling operation as discussed in the previous section, and causing a instability at lower current.

TABLE II COMPARISON DATA OF TESTED SR MAGNETS

| **SR Magnet** / Strand | Imax /Bc @4.5K | Imax /Bc @2.2K |
|---|---|---|
| **SR03** / $Nb_3Sn$, RRP | 27.5 kA // 10.9 T | 30 kA // 11.9T |
| **SR06** / $Nb_3Sn$, RRP | 28.6 kA // 10.3 T | 26.6 kA // 9.7 T |
| **SR07** / $Nb_3Al$, F4 | 24.5 kA // 9.7 T | 27 kA // 10.7T |

## B. *Training of SR Magnets*

Another remarkable thing about the SR07 $Nb_3Al$ magnet is that it did not have an extensive training, while some $Nb_3Sn$ magnets had extensive training, as is shown in Fig. 12. This may be due to the extra hardness of the $Nb_3Al$ strands, and cracking of the epoxy might be prevented. This will be an advantage for the $Nb_3Al$ magnets when operating a large number of high field magnets on a large scale.

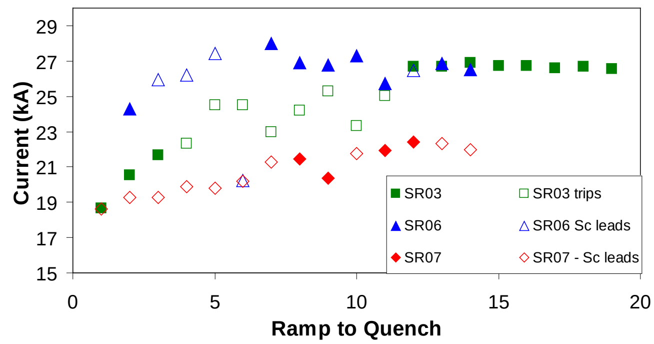


Fig. 12. Initial training curves of Small Racetrack Magnets, SR07 ($Nb_3Al$), and SR03 and SR06 (both $Nb_3Sn$) at 4.5 K. All magnets started at 19 kA (all tripping). The filled marks represent quench points. Unfilled marks show tripping due to heating of the copper leads.

## VI. DISCUSSION

The high current density $Nb_3Sn$ strands, made with the internal tin method, have been applied successfully for high field solenoid magnets, including large scale MRI and NMR magnets. They have been used successfully, usually as strands.

For high field accelerator magnets, we have to make Rutherford cables for high current applications. In this process we compress the $Nb_3Sn$ strands, causing deformed and/or damaged subelements. When the subelements are damaged, it causes tin leakage and in the worst case shears subelements. Even in the slightly deformed case, the distance between the tin and Niobium will be increased greatly. It will become difficult to have an optimized heat treatment time for the whole coil, resulting in reduced Ic values.

As the first suggestion, we should design coils using rectangular Rutherford cables, avoiding heavily key-stoned Rutherford cables. Another suggestion is to make Rutherford cables with rounded edges, to avoid damaging the edge strands. This effect is being studied, using computer simulation, as shown in Fig. 13 [15].

The present Jc value of RHQT $Nb_3Al$ is about 1500 A/mm$^2$ at 4.2 K and 12 Tesla. It is lower by about 40 %, compared with the Jc value 2500 A/mm$^2$ of RRP. RRP strands are quoted to have their Jc value from 2,000 to 3,000 A/mm$^2$. But with extra tin content, it is harder to make reliable Rutherford cables with $Nb_3Sn$ strands beyond 2500 A/mm$^2$. Event at that

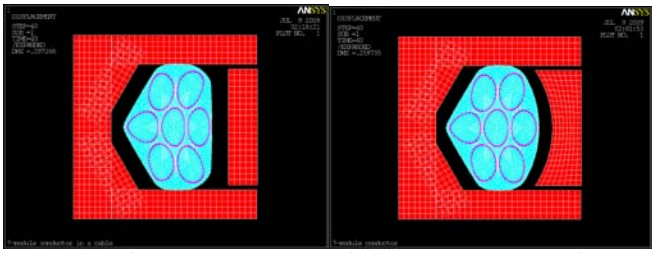

Fig. 13. Deformation simulations of the right end strand of a $NB_3Sn$ Rutherford cable with the flat end (left), and with the round end (right).

value, the extracted strands show degradation about 20 % in short sample data due to Rutherford cabling [7]. The $Nb_3Sn$ strands experience degradation of about 15 % at the compressive stress of 100 MPa. Altogether, $Nb_3Sn$ strands may experience about 35 % degradation in magnets. In very high field magnets, this degradation may be even larger.

While the $Nb_3Al$ cables are a little harder to make than $Nb_3Sn$ cables, there is no degradation due to Rutherford cabling operation and there is practically no degradation due to the compressive force up to 210 MPa. In this sense, even now, $Nb_3Al$ strands can be attractive for high field magnets with high stress level.

## VII. Conclusion

The magnet SR07 is the first stable high field magnet built using the fully copper stabilized Ta matrix $Nb_3Al$ strand. It did not have any training, and achieved 100 % short sample level. It is also completely free from low field instability both at 4.5 and 2.2 K operation.

The $Nb_3Al$ magnet SR07 did not show excessive training. This is very practical advantage of the $Nb_3Al$ magnets, because the presently tested $Nb_3Sn$ magnets are all going through more than 10 training quenches to achieve its ultimate field values.

With the successful and stable operation of the small racetrack magnet SR07, the feasibility of the $Nb_3Al$ strands and its Rutherford cables for their application in high field magnets is now established. We now know that $Nb_3Al$ Rutherford cables can be made without any problem.

There are still more to be done in the development of $Nb_3Al$ strands. Its current density should be increased, and its cost should be decreased. But we can expect that its application for practical magnets will be developed in the near future.

$Nb_3Al$ strands and Rutherford cables have many advantages over the $Nb_3Sn$ strand and cables. They have higher strain tolerance, possibility of smaller filament diameters, much less time needed for heat treatment, and no leakage problem, which is a persistent problem with cabled $Nb_3Sn$ strands.

There will be some special applications for the $Nb_3Al$ strands and cables. They could be developed especially for applications with much finer filament size in higher field and higher stressed applications beyond $Nb_3Sn$ usage.

## Acknowledgment

The authors would like to thank all of the technical staff at the Technical Division of Fermilab and at NIMS for their technical expertise during the Rutherford cable fabrication, and SR magnets fabrication as well as testing them.

## References

[1] A. Kikuchi, R. Yamada, E. Barzi, M. Lamm, T. Takeuchi, D. Turrioni, and A.V. Zlobin, "Cu Stabilized $Nb_3Al$ Strands for the High Field Accelerator Magnet," *IEEE Trans. Appl. Supercond*., vol. 18, pp. 1026-30, 2008.

[2] R. Yamada, A. Kikuchi, G. Chlachidze, G. Ambrosio, N. Andreev, E. Barzi, R. Carcagno, V.V. Kashikin, S. Kotelnikov, M. Lamm, I. Novitski, D. Orris, C. Sylvester, T. Takeuchi, M. Tartaglia, J.C. Tompkins, D. Turrioni, M. Wake, A. Yuan and A.V. Zlobin, "Quench Tests and FEM Analysis of $Nb_3Al$ Rutherford Cables and Small Racetrack Magnets," *IEEE Trans. Appl. Supercond*., vol. 19, pp. 1116-20, 2009.

[3] R. Yamada, M. Wake, A. Kikuchi and V. Velev," Magnetization, Low Field Instability and Quench of RHQT $Nb_3Al$ Starands," *IEEE Trans. Appl. Supercond*., vol. 19, pp. 2477-80, 2009.

[4] A. Kikuchi, R. Yamada, E. Barzi, M. Kobayashi, M. Lamm, K. Nakagawa, K. Sasaki, T. Takeuchi, D. Turrioni, and A. V. Zlobin, "Characteristics of Cu Stabilized Nb3Al Strands with Low Cu Ratio," *IEEE Trans. Appl. Supercond*., vol. 19, pp. 2678-81, 2009.

[5] A.V. Zlobin, N. Andreev, E. Barzi, R. Bossert, G. Chlachidze, V.S. Kashikhin, V.V. Kashikhin, M. Lamm, I. Novitski, M. Tartaglia, J.C. Tompkins, D. Turrioni, R. Yamada, "Testing of $Nb_3Sn$ Quadrupole Coils using Magnetic Mirror Structures," Presented at CEC-ICMC2009, 2009.

[6] G. Chlachidze, G. Ambrosio, N. Andreev, E. Barzi, R. Bossert, H. Carcagno, V.S. Kashikhin, VV. Kashikhin, M.J. Lamm, F.Nobrega, I. Novitski, D. Orris, C. Sylvester, M. Tartaglia, J.C. Tompkins, D. Turrioni, G. Velev, R.Yamada and A.V. Zlobin, "Quench Performance of a 4-m Long $Nb_3Sn$ Shell-Type Dipole Coil," *IEEE Trans. Appl. Supercond*., vol. 19, pp. 1217-20, 2009.

[7] E. Barzi, N. Andreev, M.Bossert, V.V. Kashikhin, D. Turrioni, A. Rusy, R. Yamada. And A.V. Zlobin, "Development and Study of $Nb_3Sn$ Strands and Cables for High-Field Accelerator Magnets," Presented at CEC-ICMC2009, 2009.

[8] J.A. Parrell, Y. Zhang, M. B. Field, P. Cisek, and S. Hong, "High Field $Nb_3Sn$ Conductor Development at Oxford Superconducting Technology," *IEEE Trans. Appl. Supercond.*, vol.13, pp.3470–73, 2003.

[9] E. Barzi, G. Ambrosio, N. Andreev, R. Bossert, R. Carcagno, S. Fehre, V.S. Kashikhin, V.V. Kashikhin, M. Lamm, F. Nobrega, I. Novitski, Y. Pishalnikov, C. Sylvester, M. Tartaglia, D. Turrioni, R. Yamada, A.V. Zlobin, M. Field, S. Hong, J. Parrell and Y. Zhang, "Performance of $Nb_3Sn$ RRP Strands and Cables Based on 108/127 Stack Design," *IEEE Trans. Appl. Supercond*., vol. 17, pp. 2718-21, 2007.

[10] R. Yamada and M. Wake, "Quench Problems of $Nb_3Sn$ Cosine Theta High Field Dipole Magnets," *IEEE Trans. Appl. Supercond*., vol. 15, pp. 1140-43, 2005.

[11] M.D. Sumption, M. Susner, E.W. Collins, D.R. Dietderich, E. Barzi, D. Turrioni, R. Yamada and A.V. Zlobin," Effect of Cable Edge Deformation on RRR and Magnetization of Strands Extracted From $Nb_3Sn$ Rutherford-Type Cables," *IEEE Trans. Appl. Supercond*., vol. 19, pp. 2481-85, 2009.

[12] R. Yamada, A. Kikuchi, M. Tartaglia, G. Ambrosio, N. Andreev, E. Barzi, R. Carcagno, S. Feher, V.V. Kashikin, S. Kotelnikov, M. Lamm, I. Novitski, D. Orris, Y. Pischalnikov, T. Takeuchi, J.C. Tompkins, D. Turrioni, M. Wake, R. Wands, J. Xiao, M. Yu, A. Yuan and A.V. Zlobin "Quench Tests of $Nb_3Al$ Small Racetrack Magnets", *IEEE Trans. Appl. Supercond*., vol. 18 , pp. 1039-42, 2008.

[13] S. Feher, G. Ambrosio, N. Andreev, E. Barzi, B. Bordini, R. Carcagno, V.I. Kashikin, V.V. Kashikin, M.J. Lamm, I. Novitski, D. Orris, Y. Pischalnikov, C. Sylvester, M. Tartaglia, R. Yamada and A.V. Zlobin "Cable Testing for Fermilab's High Hield Magnets using Small Racetrack Coils", *IEEE Trans. Appl. Supercond*., vol. 15, pp. 1550-53, 2005.

[14] G. Chlachidze, R. Yamada, A. Kikuchi, G. Ambrosio, R. Carcagno, S. Kotelinikov, F. Lewis, D. Orris, C. Sylvester, M. Tartaglia, J.C. Tompkins and A.V. Zlobin, "SR07 Small Racetrack Magnet Test Summary" TD-08-066, Fermilab Internal Report, July 29, 2008.

[15] Refer to the on-line demonstration of Quench Simulation of SR magnets at http://research.kek.jp/people/wake/SR_magnet_Quench/